Zinc-bearing dust derived non-toxic mixed iron oxides as magnetically recyclable photo-Fenton catalyst for degradation of dye

Jian-ming Gao, ShuJia Ma, Zongyuan Du, Fangqin Cheng and Peng Li

ABSTRACT

In this paper, comprehensive utilization of hazardous zinc-bearing dust for preparation of non-toxic mixed iron oxides as a magnetically recyclable photo-Fenton catalyst for degradation of dye by a facile solid state reaction process was proposed. The as-prepared samples were characterized by X-ray diffraction (XRD), Raman spectra, ultraviolet and visible (UV-Vis) spectra and Physical Property Measurement System (PPMS), and the degradation performance of as-prepared catalysts was also tested and analyzed. The results show that spinel ferrite coexisting with or without Fe_2O_3 was the predominant phase in the as-prepared samples, which were confirmed by Raman analysis. The as-prepared samples presented high degradation efficiency (about 90%) of rhodamine B (RhB) in the presence of hydrogen peroxide (H_2O_2) with visible light irradiation, owing to the synergistic effect of photocatalyst reaction and Fenton-like catalyst reaction during the degradation process. The mixed iron oxides also presented stable structure and exhibited excellent reusability with a degradation efficiency of 87% after the fifth cycle of reuse. Importantly, the heavy metals in the zinc-bearing dust could be fixed in the stable spinel structure. This paper could provide a simple approach for comprehensive utilization of zinc-bearing dust to synthesize non-toxic mixed iron oxides as a magnetically recyclable photo-Fenton catalyst for degradation of dye.

Key words | dye degradation, magnetically recyclable, mixed iron oxide, photo-Fenton catalyst, zinc-bearing dust

Jian-ming Gao (corresponding author)
ShuJia Ma
Zongyuan Du
Fangqin Cheng
State Environmental Protection Key Laboratory of Efficient Utilization Technology of Coal Waste Resources, Shanxi Collaborative Innovation Center of High Value-added Utilization of Coal-related Wastes,
Shanxi University,
Taiyuan 030006,
China
E-mail: *gaojianming@sxu.edu.cn*

Peng Li
Shagang School of Iron and Steel,
Soochow University,
Suzhou, 215021,
China

HIGHLIGHTS

- Non-toxic mixed iron oxides were prepared from hazardous zinc-bearing dust.
- Mixed iron oxides could be used as a magnetically recyclable photo-Fenton catalyst.
- The catalyst exhibited degradation efficiency of 85% after the fifth cycle of reuse.
- Heavy metals in the zinc-bearing dust could be fixed in the stable spinel structure.

INTRODUCTION

The contamination caused by organic dyes has been of great concern due to the toxicity to humans, and various physical, biological and chemical methods including adsorption (Jiang *et al.* 2019; Zhou *et al.* 2019), membrane separation (Ramlow *et al.* 2017), and oxidation (Liu *et al.* 2021) have been developed for the treatment of dye wastewater. Among these methods, advanced oxidation processes (AOPs) based on the technology of Fenton reaction are potentially applied in industrial wastewater treatment to degrade recalcitrant organic pollutants, which are cost effective and environmentally friendly (Neyens & Baeyens 2003; Zapata *et al.* 2009; Gligorovski *et al.* 2015). The technology is based on the generation of powerful hydroxyl radicals, •OH, which can oxidize and mineralize organic pollutants in wastewater. The generation process involves simple

doi: 10.2166/wst.2020.590

reactions as follows:

$$Fe^{2+} + H_2O_2 \rightarrow Fe^{3+} + OH^- + \bullet OH \quad (1)$$

$$Fe^{3+} + H_2O_2 \rightarrow Fe^{2+} + H^+ + HO_2\bullet \quad (2)$$

However, generation of large amounts of iron-bearing sludge and low reaction pH value during the processes limited the wide application of homogeneous Fenton reaction. Consequently, heterogeneous Fenton-like catalysts, such as nano-flake Fe-SC hybrid, Cu-impregnated zeolite Y, sulfur-modified iron oxide, and amorphous $Fe_{78}Si_9B_{13}$ alloy etc. have been synthesized and confirmed the Fenton-like reaction on the solid-liquid interface (Du *et al.* 2016; Jia *et al.* 2016; Kong *et al.* 2016).

Mixed iron oxides, spinel ferrites MFe_2O_4 (M = Ni, Mn, Co, Mg, Cu, Zn, etc.), have been applied as heterogeneous catalysts in the Fenton-like processes, which exhibit unique structural, magnetic properties and catalytic performance (Ahmed & Ahmaruzzaman 2015; Kefeni *et al.* 2017; Vinosha *et al.* 2017). Liu *et al.* (2012) successfully synthesized magnetic $NiFe_2O_4$ by the hydrothermal method, and as-prepared nickel ferrite exhibited photo-Fenton catalytic features for organic pollutants in the presence of oxalic acid. Seven cyclic tests for rhodamine B degradation demonstrated that the catalyst is stable and highly active with a degradation efficiency of above 90%. Highly ordered mesoporous $CuFe_2O_4$ was successfully obtained and proposed as a heterogeneous Fenton-like catalyst (Zhang *et al.* 2014). The $CuFe_2O_4$ catalyst presented low metal leaching (<1 ppm) even in acidic conditions and retained high catalytic activity (3.75% decrease) after six cycles of reuse. Besides, many studies demonstrated that spinel ferrites presented excellent catalytic activity in Fenton-like reaction system, such as $ZnFe_2O_4$, $CoFe_2O_4$, $MgFe_2O_4$, and $Zn_xCo_{1-x}Fe_2O_4$ (Su *et al.* 2012; Feng *et al.* 2013; Shahid *et al.* 2013; Cai *et al.* 2016). Moreover, it is confirmed that for some metal elements, such as Cr, Mn, Ti or V, substitution into the spinel structure can be facilitated to improve the catalytic activity of the spinel ferrite-based Fenton-like catalysts (Zhong *et al.* 2014). Furthermore, they are all inverse spinels with excellent stability, and toxic ions could be stably fixed in spinel ferrites (Chen *et al.* 2011; Tu *et al.* 2012), demonstrating that multi-metal doped spinel ferrites could be used as magnetically recyclable Fenton-like catalysts for organic pollutant degradation.

Zinc-bearing dust, generated during the iron and steel production process, is classified as hazardous solid waste that contains various heavy metals, such as Zn, Mn, Fe, Pb, Cr etc. Currently, much effort was focused on the extraction and recycling of valuable metals from zinc-bearing dust using various complex pyrometallurgical and/or hydrometallurgical processes, leading to not only environmental pollution problems but also low recovery of valuable metals (Kukurugya *et al.* 2015; Lin *et al.* 2017; Zhang *et al.* 2017a). Unfortunately, few works have studied comprehensive utilization of valuable metals in zinc-bearing dust. Notably, Zn, Mn, Fe, Cr etc. in the zinc-bearing dust are the main chemical compositions of spinel ferrites (Gao & Cheng 2018a, 2018b), suggesting that zinc-bearing dust could be used as raw material for preparation of spinel ferrites as magnetically recyclable heterogeneous Fenton-like catalysts. Besides, the gap vacancy and lattice defects in spinel ferrites could provide structural conditions for metal substitution into the spinel structure, implying that it is reasonable to synthesize multi-metal doped spinel ferrites from zinc-bearing dust. Furthermore, heavy metal ions easily dissolved in water from zinc-bearing dust could be stably fixed in the stable spinel structure, which might be facilitated to improve the catalytic activity of the spinel ferrite-based Fenton-like catalysts. In short, comprehensive utilization of hazardous zinc-bearing dust for preparation of non-toxic mixed iron oxides as magnetically recyclable photo-Fenton catalyst for degradation of dye meets the requirements of a resource-saving and environment-friendly society.

So far, some mixed iron oxides as heterogeneous Fenton-like catalysts have been successfully synthesized from solid waste or natural minerals. Cao *et al.* (2017) reported that zinc ferrite catalysts for efficient degradation of organic dye were fabricated by the calcination of electroplating sludge, and the as-prepared catalysts exhibited excellent MB decolorization efficiency (about 85%) in a UV/H_2O_2 system. Zhang *et al.* (2017b) provided a novel method for the reuse of iron-containing Fenton sludge and nickel ferrite was synthesized as an efficient catalyst in the heterogeneous Fenton process. A phenol degradation efficiency of about 95% could be obtained in the presence of both nickel ferrite and H_2O_2. Furthermore, multi-metal co-doped magnesium ferrite was successfully synthesized from saprolite laterite ore by Diao *et al.* (2017), and used as heterogeneous photo-Fenton like catalyst for dye degradation. The as-prepared ferrite exhibited excellent catalytic activity with a degradation efficiency of 96.8%, which is more competitive compared to the catalysts prepared from chemical reagents. That is to say, it is feasible to obtain excellent heterogeneous Fenton-like catalysts from solid waste or liquid waste.

In this paper, multi-metal doped spinel ferrites were synthesized from zinc-bearing dust by the facile solid state reaction method. The structure and magnetic properties of as-prepared mixed iron oxides were characterized and discussed. Then the as-prepared ferrites were used for the degradation of organic pollutants by photo-Fenton reaction, and the effects of degradation conditions and Zn/Fe molar ratio on the degradation efficiency of rhodamine B (RhB) were investigated. Simultaneously, the dissolution characteristics of heavy metals in the zinc-bearing dust and as-prepared spinel ferrites were also tested to verify the environmental security of zinc-bearing dust-derived mixed iron oxide photo-Fenton catalysts. Finally, the possible catalytic mechanism for degradation of RhB using zinc-bearing dust-derived mixed iron oxides as photo-Fenton catalysts a proposed. This paper might provide a simple approach for comprehensive utilization of zinc-bearing dust in a green pollution-free method.

EXPERIMENTAL PROCEDURE

Materials and reagents

The zinc-bearing dust using in this study was collected from a stainless steel plant in China, and the main chemical compositions of the zinc-bearing dust are summarized in Table 1. In the zinc-bearing dust, spinel ferrites including $ZnFe_2O_4$ and Fe_3O_4, calcite ($CaCO_3$) and quartz (SiO_2) are the main phases as reported in the literature (Gao & Cheng 2018a). All the reagents used in this study are of analytical grade and used without any treatment.

Sample preparation

Using the facile solid state reaction method, the mixed iron oxides were prepared by the following procedure. Firstly, zinc-bearing dust was dried at 105 °C for 12 h and ground to a particle size smaller than 75 μm. Then, 5.0 g zinc-bearing dust was mixed with a certain amount of ZnO reagent, and the mixture was ground adequately in an agate mortar to form a uniform powder. Finally, the uniform powder was transferred into a corundum crucible, and calcinated at 900 °C for 60 min with a heating rate of 10 °C·min^{-1} in a muffle furnace to obtain mixed iron oxide. In this paper, to investigate the effect of Zn/Fe molar ratio on zinc ferrite ($ZnFe_2O_4$) based photo-Fenton catalysts synthesized from zinc-bearing dust, the mass ratios of 2:0.4, 2:0.6 and 2:0.8 were chose, and the molar ratio of Zn to Fe in the dust and the mixture of zinc-bearing dust and ZnO addition are calculated and listed in Table 1. The as-prepared mixed iron oxides with mass ratios of 2:0.4, 2:0.6 and 2:0.8 were labeled as ZF1, ZF2 and ZF3, respectively.

Degradation experiments

The as-prepared mixed iron oxides were used as a Fenton-like catalyst for the degradation of RhB at a constant temperature of 25 °C. A 500 W Xe lamp with 420 nm cutoff filter was used as the visible light source. In the degradation experiment, 0.2 g as-prepared mixed iron oxides was first dispersed in 200 mL of the RhB aqueous solution (10 mg/L) in a dark environment for 30 min to ensure that the RhB reached an adsorption equilibrium on the surface of the photocatalysts at a pH value of 4.0. Then a solution containing H_2O_2 (2.0 mmol/L) was added in the aqueous solution, and reacted with magnetic stirring. During the irradiation process, 5 mL of the suspension was collected every 30 min and centrifuged for subsequent RhB absorbance analysis. The remaining RhB dye concentration was detected by ultraviolet-visible (UV-Vis) spectrophotometer at a wavelength of 554 nm (Bhargava *et al.* 2016). The degradation efficiency η was calculated according to Equation (3).

$$\eta = \frac{C_o V_o - C_e V_e}{C_o V_o} \times 100\% \quad (3)$$

Table 1 | Main chemical compositions and molar ratio of Zn to Fe of zinc-bearing dust and mixtures with different mass ratios used in this study wt.%

Chemical compositions	Fe_2O_3	ZnO	MnO_2	MgO	CuO	PbO	Cr_2O_3	CaO	SiO_2	Molar ratio of Zn to Fe
Zinc-bearing dust	64.1	10.4	0.8	1.7	0.3	1.3	0.5	1.0	5.3	0.32:2
2:0.4	64.1	30.4	0.8	1.7	0.3	1.3	0.5	1.0	5.3	0.93:2
2:0.6	64.1	40.4	0.8	1.7	0.3	1.3	0.5	1.0	5.3	1.25:2
2:0.8	64.1	50.4	0.8	1.7	0.3	1.3	0.5	1.0	5.3	1.54:2

where C_o and C_e represent the concentration of RhB dye in the initial solution and after the degradation process, respectively, g·mL^{-1}; V_o and V_e are the volumes of the initial RhB dye solution and after the degradation process, respectively, mL.

Toxicity leaching test

To evaluate the chemical stability and ensure the stability toward metal ion leaching from as-prepared mixed iron oxides to the solution under the reaction conditions, the Toxicity Characteristic Leaching Procedure (TCLP) (1311) formulated by the US Environmental Protection Agency (US EPA) (Sebag *et al.* 2009) was adopted and distilled water with a pH value of 2.88 was chosen as the leaching agent. The test procedures were as follows: firstly, 1.0 g zinc-bearing dust or as-prepared mixed iron oxide and 20 mL leaching agent were mixed in a centrifuge tube, and the mixture was shaken at a speed of 30 rpm at 25 °C for 24 h, and then filtered to obtain the filtrate. The concentration of metal ions in the filtrate were determined by inductively coupled plasma optical emission spectrometer (ICP-OES).

Analysis and characterization

The mineral phase compositions of as-prepared samples were recorded by X-ray diffractometer (XRD, Rigaku, Cu Kα radiation, $\lambda = 0.15406$ nm) at a scanning rate of 0.02 deg·s^{-1} at the diffraction angle (2θ) 10–90° with a voltage of 40 kV and 40 mA. Room temperature Raman spectra of as-prepared samples were tested using a Raman spectrometer equipped with an Ar^+ laser (532 nm, 10 mW) excitation source and a CCD detector. The UV-Vis spectra of as-prepared samples were measured with an UV-Vis spectrophotometer (Hitachi U-3010). Physical Property Measurement System (PPMS, America, 9 T (EC-II)) was explored to test the magnetic properties of as-prepared samples with the applied magnetic field varying from −10,000 to 10,000 Oe.

RESULTS AND DISCUSSION

Characterization of mixed iron oxides

The XRD patterns of as-prepared samples with different mass ratios of zinc-bearing dust to ZnO addition of 2:0.4, 2:0.6, and 2:0.8 is shown in Figure 1. According to the PDF card, peaks appear at 29.9°, 35.3°, 42.8°, 56.6° and 62.2° match well with PDF card 22–1022 (Franklinite, $ZnFe_2O_4$) (National Bureau of Standards 1971), which correspond to the crystal face (220), (311), (400), (511) and (440) of franklinite, respectively. Peaks appear 24.1°, 33.2°, 40.9° and 49.5° match well with PDF card 33–0664 (Hematite, Fe_2O_3) (National Bureau of Standards 1981), which correspond to the crystal face (012), (104), (113) and (024) of hematite, respectively. As can be seen from Figure 1, when the mass ratio is controlled at 2:0.4, the diffraction peaks of both spinel ferrite $ZnFe_2O_4$ and the rhombohedral structure of Fe_2O_3 were detected. With the mass ratio decreasing to 2:0.6 and 2:0.8, the intense diffraction peaks were well indexed to spinel ferrite $ZnFe_2O_4$, and the diffraction peaks of Fe_2O_3 disappeared, indicating the formation of single-phase spinel ferrite. Furthermore, with the mass ratios increasing, the diffraction peaks increased in intensity, implying that the purity and crystallinity of as-prepared samples might be improved.

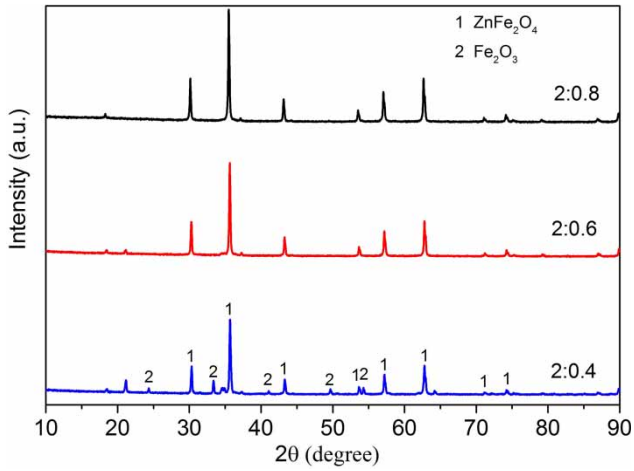

Figure 1 | XRD patterns of as-prepared samples with different mass ratios of zinc-bearing dust to ZnO addition of 2:0.4, 2:0.6, and 2:0.8.

In the Raman spectra, there are five optical Raman-active modes for spinel space group (Fd3 m), A1 g + Eg + 3T2 g. The notations A, E and T are one, two and three dimensional representations, respectively, and g represents the symmetry regarding the center of inversion. In spinel ferrites, the assignment of the Raman-active modes and the regions where they are located are given as follows:

(i) The T2 g(1) active mode located at 213–243 cm^{-1} are associated to translational movements of the whole MO_4 tetrahedral. M and O represent Metal and Oxygen, respectively.
(ii) The Eg active mode located at 334–352 cm^{-1} are related to symmetric bending vibrations of O atoms with respect to M in tetrahedral (A) sites.

(iii) The T2 g(2) active mode appearing at 478–488 cm^{-1} is ascribed to asymmetric stretching vibrations of M – O in tetrahedral sites.
(iv) The T2 g(3) active mode appearing at 540–571 cm^{-1} is assigned to asymmetric bending vibration of O atoms with respect to M in tetrahedral sites.
(v) The A1 g symmetry active mode located in the range 600–710 cm^{-1} is related to symmetric stretching vibrations of M – O in tetrahedral (A) sites. For this mode, it has been confirmed that the Raman spectrum of normal spinel ferrites is located in the 600–620 cm^{-1} region, while that of inverse spinel ferrite occurs in the 670–710 cm^{-1} region.

The as-prepared mixed iron oxides are also characterized by Raman spectra, as presented in Figure 2. It can be observed that the peaks appearing around 205, 280, 335, 475, 645 and 700 cm^{-1} were assigned to the A_{1g}, E_g, and $3T_{2g}$ Raman active modes of spinel ferrite $ZnFe_2O_4$ (Yan *et al.* 2015; Aakash *et al.* 2016), further confirming the formation of spinel ferrite. Furthermore, the $A_{1g}(1)$ mode (around 700 cm^{-1}) and $A_{1g}(2)$ mode (around 640 cm^{-1}) are the symmetric stretch of O along the Fe-O bonds and Zn-O bonds at the tetrahedral sites, respectively (Thota *et al.* 2015). With the mass ratios of zinc-bearing dust to ZnO addition decreasing from 2:0.4 to 2:0.8, the intensity of $A_{1g}(1)$ mode decreased while that of the $A_{1g}(2)$ mode increased, implying that Zn^{2+} ion substitution into spinel ferrites could cause cation redistribution. When Zn was substituted in the as-prepared spinel ferrites, Zn^{2+} ions preferred to occupy the tetrahedral (A) sites, and forced the same amount of Fe^{3+} ions to transfer to the octahedral (B) sites.

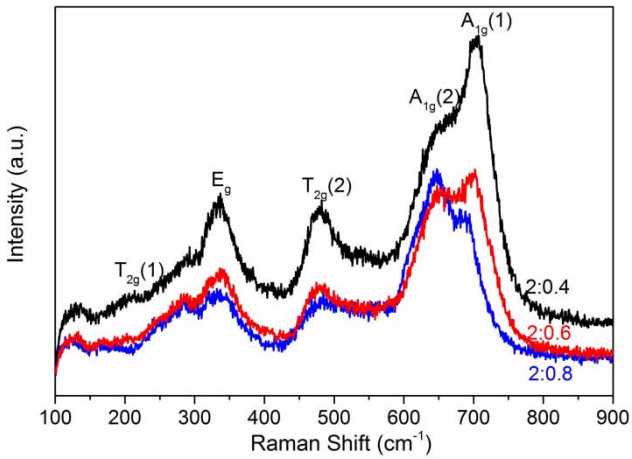

Figure 2 | Raman spectra of as-prepared samples with different mass ratios of zinc-bearing dust to ZnO addition of 2:0.4, 2:0.6, and 2:0.8.

As a photo-Fenton catalyst, it is essential to understand the optical properties of as-prepared samples, and Figure 3 presents the UV- Vis spectra of as-prepared ZF1, ZF2 and ZF3 with wavelengths ranging from 200 to 800 nm. All three samples exhibit intense absorption in a wide wavelength varying from UV to visible light with an absorption tail extending into the infrared region. The band gap (Eg) can be calculated by the Tauc's equation as follows:

$$(\partial h\upsilon)^n = A(h\upsilon - Eg) \tag{4}$$

where α is the absorption coefficient, h is the Planck's constant, υ is the frequency of light and A is a constant. The bandgap energy could be evaluated for direct ($n = 2$) and indirect ($n = 1/2$) electronic transitions determined by extrapolation of the linear regions of the Tauc's plots to zero absorption. The bandgap energy is obtained by extrapolating the tangent of the curve to x-axis as plotted in the inset. The bandgaps for ZF1, ZF2 and ZF3 are 1.92 eV, 1.94 eV and 1.96 eV, respectively, which are close to that for zinc ferrite.

The magnetic properties of as-prepared samples were measured by PPMS, and room temperature hysteresis loops are illustrated in Figure 4. All the as-prepared samples exhibit ferrimagnetism behaviors. With Zn^{2+} ion substitution content increasing (mass ratios from 2:0.4 to 2:0.8), the saturation magnetization values decreased from 33.8 emu g^{-1} to 20.3 emu g^{-1}. From the inset of Figure 4, it can be observed that the as-prepared sample could be easily separated from the reaction system by using a magnet, providing a practical approach to recycle and reuse the catalyst.

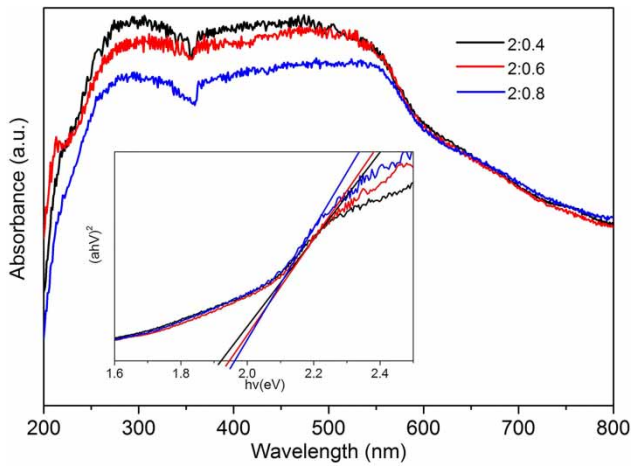

Figure 3 | UV- Vis spectra of as-prepared samples with different mass ratios of zinc-bearing dust to ZnO addition of 2:0.4, 2:0.6, and 2:0.8, inset: Tauc's plots for the calculation of bandgap.

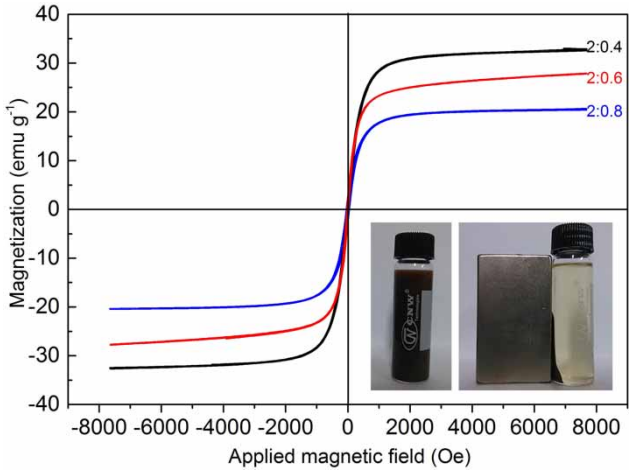

Figure 4 | Room temperature hysteresis loops of as-prepared samples with different mass ratios of zinc-bearing dust to ZnO addition of 2:0.4, 2:0.6, and 2:0.8.

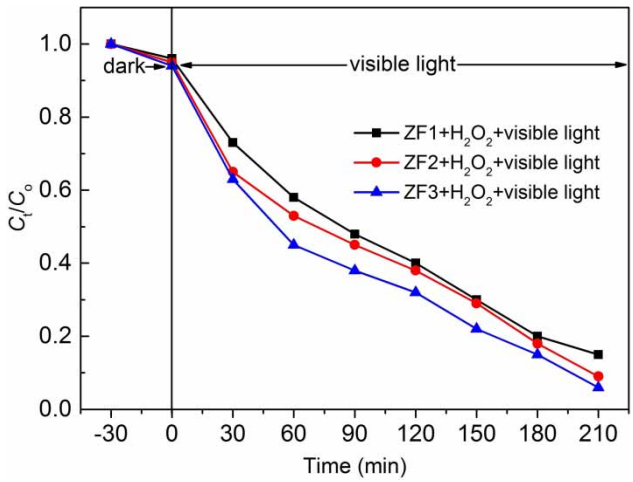

Figure 6 | Degradation efficiency of RhB using ZF1, ZF2 and ZF3 as catalysts in the H_2O_2/visible light system, the initial RhB concertation of 10 mg/L, the pH value at 4.0, 2.0 mmol/L H_2O_2, and 1 g/L catalyst dosage.

Degradation of dye

The RhB degradation experiments using as-prepared ZF1, ZF2 and ZF3 as catalysts were carried out as shown in Figures 5 and 6. Figure 5 shows the degradation efficiency of RhB using ZF2 as the catalyst under different reaction conditions. Clearly, as shown in Figure 5, the self-degradation of RhB is very weak under visible light irradiation in the absence of mixed iron oxides and H_2O_2. It can be also observed that the degradation efficiency is only 2% using H_2O_2 as the catalyst in the dark after reaction for 210 min. Under the visible light irradiation, the degradation efficiency could be improved (about 30%) using H_2O_2 as the catalyst. Using ZF2 as catalyst, the degradation efficiency is increased to 50% with the addition of H_2O_2 in the dark. However, using ZF2 as photocatalyst without the addition of H_2O_2, the degradation efficiency is about 20%, implying that ZF2 is not an efficient photocatalyst for the degradation of RhB. In the presence of H_2O_2 and with visible light irradiation, ZF2 catalyst could reach 91% RhB degradation. Such results demonstrated that zinc-bearing dust-derived mixed iron oxide ZF2 is an effective heterogeneous photo-Fenton-like catalyst for RhB degradation. Besides, the key roles of H_2O_2 addition and visible light irradiation are also indispensable in the photo-Fenton reaction system.

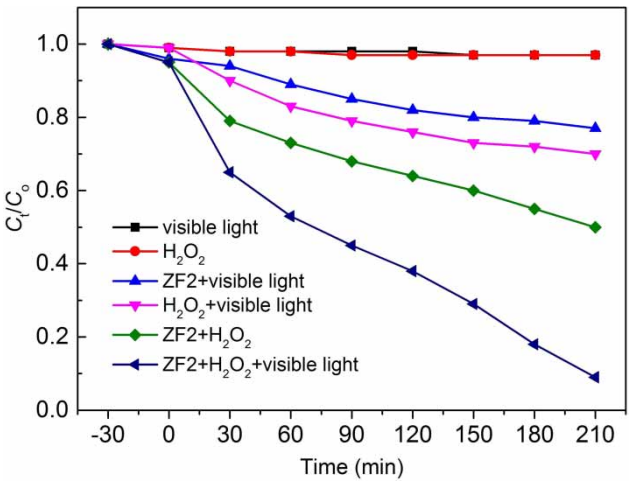

Figure 5 | Degradation efficiency of RhB using ZF2 as the catalyst under different reaction conditions.

As observed from Figure 6, the degradation of RhB for ZF1, ZF2 and ZF3 catalysts slightly increases from 91% to 95% after reaction for 210 min, which might be ascribed to the active catalytic sites increasing when more Zn^{2+} ions occupied the tetrahedral (A) sites and forced more Fe^{3+} ions to occupy the octahedral (B) sites, as discussed in Figure 2. Moreover, the required reaction time for the similar degradation of dye using as-synthesized mixed iron oxide catalysts is longer than that of some reported literatures (Cao *et al.* 2017; Diao *et al.* 2017), which might be ascribed to the relatively low catalytic activity of as-synthesized mixed iron oxide catalysts resulting from high synthesis temperature as analyzed in the literature (Cao *et al.* 2017; Ismael 2021).

To further identify the main active oxidative species in the visible light/ZF2/H_2O_2 system, the degradation experiments with the addition of hydroxyl radicals •OH scavenger (tert-butanol (TBA)) and the holes scavenger (Ethylene Diamine Tetraacetic Acid (EDTA)) were carried out and the results are shown in Figure 7. As observed in Figure 7, with the addition of EDTA (1 mM), the degradation of RhB decreases from 91% to 60%, implying that

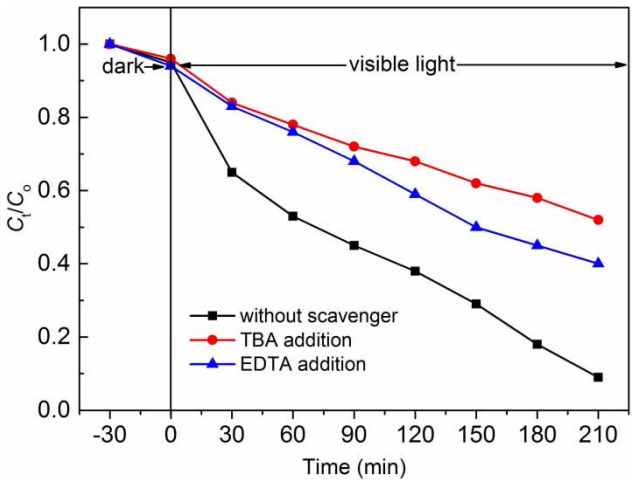

Figure 7 | Influence of radical scavengers on degradation efficiency of RhB using ZF2 as catalysts in the H_2O_2/visible light system, the initial RhB concentration of 10 mg/L, the pH value of 4.0, 2.0 mmol/L H_2O_2, and 1 g/L catalyst dosage.

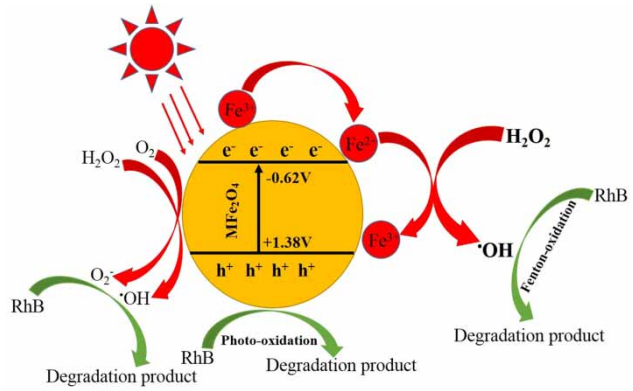

Figure 8 | Suggested mechanism for degradation of RhB by Zinc-bearing dust derived mixed iron oxides photo-Fenton catalysts.

EDTA have some effects on the degradation of RhB. When TBA was added in the system, the degradation of RhB decreases from 91% to 48%, indicating that TBA (1 M) greatly inhibited the degradation reaction. As a result, the generated hydroxyl radicals •OH played a key role in degradation of RhB and the generated electrons were of great importance for the degradation process.

Generally, in a Fenton reaction system, Fe^{2+} ions can be oxidized by H_2O_2 to generate powerful hydroxyl radicals •OH, which have a standard potential of 2.8 V (Kostedt *et al.* 2005). They can oxidize and mineralize organic pollutants in wastewater. In the H_2O_2 system, few hydroxyl radicals •OH could be generated and resulted in low degradation efficiency. However, with visible light irradiation, hydroxyl radicals •OH can be yielded in the H_2O_2 system, leading to the improvement of degradation efficiency. Using the mixed iron oxides as Fenton-like catalyst in the presence of H_2O_2, the plus two (+2) and three (+3) Fe ions could be oxidized by H_2O_2, and lots of hydroxyl radicals •OH were produced (Munoz *et al.* 2015). As a result, the degradation efficiency could be obviously increased. Furthermore, in the presence of H_2O_2 with visible light irradiation, the as-prepared mixed iron oxides exhibited enhanced RhB degradation performance, implying that visible light irradiation is essential for effective dye degradation. The results might be ascribed to the generation of hydroxyl radicals •OH being accelerated by visible light irradiation, and the synergistic effect of the photocatalyst reaction and Fenton-like catalyst reaction. Figure 8 shows the proposed mechanism for degradation of RhB using zinc-bearing dust-derived mixed iron oxides as photo-Fenton catalysts.

Catalyst stability and reusability

As known, many heavy metals such as Zn, Mn, Cu, Pb, Cr are in the zinc-bearing dust. It is necessary to ensure security and stability towards hazardous metal leaching from as-prepared mixed iron oxides into the solutions under the reaction conditions. The hazardous metal leaching characteristics of zinc-bearing dust and as-prepared mixed iron oxide samples were tested according to the TCLP process, and the results are listed in Table 2. It can be found that

Table 2 | Metal ion concentrations in the solutions leached from zinc-bearing dust and as-prepared ZF1, ZF2 and ZF3

	Metal ion concentration (mg/L)							
Samples	**Fe**	**Zn**	**Mn**	**Cu**	**Pb**	**Cr**	**Mg**	**Ca**
Raw dust	12.23 ± 0.5	30.05 ± 0.6	0.92 ± 0.2	0.33 ± 0.1	12.05 ± 0.3	10.11 ± 0.3	0.63 ± 0.1	0.54 ± 0.1
ZF1	0.12 ± 0.02	0.30 ± 0.08	0.18 ± 0.03	0.09 ± 0.02	0.27 ± 0.05	0.26 ± 0.04	0.26 ± 0.05	0.06 ± 0.02
ZF2	0.07 ± 0.02	0.26 ± 0.05	0.07 ± 0.02	0.08 ± 0.02	0.13 ± 0.02	0.15 ± 0.03	0.29 ± 0.05	0.09 ± 0.02
ZF3	0.06 ± 0.01	0.38 ± 0.06	0.24 ± 0.03	0.06 ± 0.02	0.11 ± 0.02	0.07 ± 0.02	0.23 ± 0.05	0.11 ± 0.02
Maximum limit (Wang *et al.* 2017)	–	4	2	2	0.5	0.5	–	–

heavy metals leaching from zinc-bearing dust to the solution is serious, and most of the heavy metal concentrations are above the maximum limit; however, the heavy metals leaching from as-prepared samples are very limited (far below the maximum limit), implying that heavy metals could be fixed and doped in the stable spinel structure during the facile solid state calcination process, as reported by Chen *et al.* (2011).

Recovery and reusability are important aspects of a resource-saving and environment-friendly catalyst for practical application in wastewater treatment. The reusability of as-prepared ZF2 was studied by a five-cycle degradation of RhB under identical reaction conditions as plotted in Figure 9. The degradation efficiency was slightly decreased from 91% to 87%, implying that zinc-bearing dust-derived mixed iron oxides were stable during the reaction and could be reusable catalysts for degradation of dye. In general, zinc-bearing dust-derived mixed iron oxides could be easily separated and reused as heterogeneous photo-Fenton-like catalysts.

CONCLUSIONS

In conclusion, non-toxic mixed iron oxides as the magnetically recyclable photo-Fenton catalyst for degradation of dye were synthesized from zinc-bearing dust using a facile solid state reaction method. In the as-prepared samples, spinel ferrite coexisting with or without Fe_2O_3 was the predominant phase. The as-prepared mixed iron oxides exhibited excellent degradation efficiency (above 90%) of RhB in the presence of 2.0 mmol/L H_2O_2 and with visible light irradiation for 210 min when the initial RhB concertation is 10 mg/L and the pH value is controlled at 4.0, owing to the synergistic effect of the photocatalyst reaction and Fenton-like catalyst reaction during the degradation process. When more Zn^{2+} ions occupied the tetrahedral (A) sites and forced more Fe^{3+} ions to occupy the octahedral (B) sites, the active catalytic sites were increased, and the degradation efficiency was increased accordingly. Moreover, heavy metals in the zinc-bearing dust were fixed stably in the spinel structure, and the as-prepared samples presented excellent reusability with a degradation efficiency of 87% after the fifth cycle of reuse. This work paves a green pathway towards the comprehensive utilization of hazardous solid waste to produce high value-added material product.

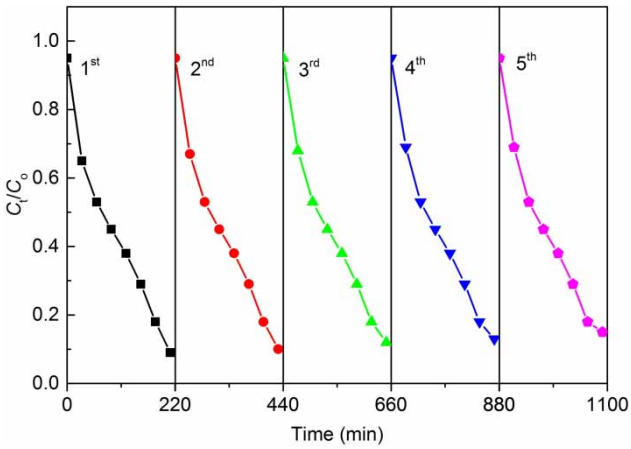

Figure 9 | Cyclic degradation efficiency of RhB using ZF2 as the catalyst in the H_2O_2/visible light system, the initial RhB concertation of 10 mg/L, the pH value at 4.0, 2.0 mmol/L H_2O_2, and 1 g/L catalyst dosage.

ACKNOWLEDGEMENTS

The work was financially supported by the National Natural Science Foundation of China (Nos. 51804192), the National Key R&D Program of China (No. 2017YFB0603102), Shanxi Province Applied Basic Research Project (No. 201801D221325), Xiangyuan Country Comprehensive Utilization Science and Technology of Solid Waste Research Projects (No. 2018XYSDJS-04).

DATA AVAILABILITY STATEMENT

All relevant data are included in the paper or its Supplementary Information.

REFERENCES

Aakash, Choubey, R., Das, D. & Mukherjee, S. 2016 Effect of doping of manganese ions on the structural and magnetic properties of nickel ferrite. *Journal of Alloys and Compounds* **668**, 33–39.

Ahmed, M. J. K. & Ahmaruzzaman, M. 2015 A facile synthesis of Fe_3O_4-charcoal composite for the sorption of a hazardous dye from aquatic environment. *Journal of Environmental Management* **163**, 163–173.

Bhargava, A., Jain, N., Khan, M. A., Pareek, V., Dilip, R. V. & Panwar, J. 2016 Utilizing metal tolerance potential of soil fungus for efficient synthesis of gold nanoparticles with superior catalytic activity for degradation of rhodamine B. *Journal of Environmental Management* **183**, 22–32.

Cai, C., Zhang, Z. Y., Liu, J., Shan, N., Zhang, H. & Dionysiou, D. D. 2016 Visible light-assisted heterogeneous Fenton with $ZnFe_2O_4$ for the degradation of Orange II in water. *Applied Catalysis B Environmental* **182**, 456–468.

Cao, Z. B., Zhang, J., Zhou, J. Z., Ruan, X. X., Chen, D., Liu, J. Y., Liu, Q. & Qian, G. R. 2017 Electroplating sludge derived zinc-ferrite catalyst for the efficient photo-Fenton degradation of dye. *Journal of Environmental Management* **193**, 146–153.

Chen, D., Mei, C. Y., Yao, L. H., Jin, H. M., Qian, G. R. & Xu, Z. P. 2011 Flash fixation of heavy metals from two industrial wastes into ferrite by microwave hydrothermal co-treatment. *Journal of Hazardous Materials* **192**, 1675–1682.

Diao, Y. F., Yan, Z. K., Guo, M. & Wang, X. D. 2017 Magnetic multi-metal co-doped magnesium ferrite nanoparticles: an efficient visible light-assisted heterogeneous Fenton-like catalyst synthesized from saprolite laterite ore. *Journal of Hazardous Materials* **344**, 829–838.

Du, J. K., Bao, J. G., Fu, X. Y., Lu, C. H. & Kim, S. H. 2016 Mesoporous sulfur-modified iron oxide as an effective Fenton-like catalyst for degradation of bisphenol A. *Applied Catalysis B Environmental* **184**, 132–141.

Feng, X., Mao, G. Y., Bu, F. X., Cheng, X. L., Jiang, D. M. & Jiang, J. S. 2013 Controlled synthesis of monodisperse $CoFe_2O_4$ nanoparticles by the phase transfer method and their catalytic activity on methylene blue discoloration with H_2O_2. *Journal of Magnetism & Magnetic Materials* **343**, 126–132.

Gao, J. M. & Cheng, F. Q. 2018a Effect of metal substitution on the magnetic properties of spinel ferrites synthesized from zinc-bearing dust. *Journal of Superconductivity and Novel Magnetism* **31**, 1965–1970.

Gao, J. M. & Cheng, F. Q. 2018b Facile synthesis of spinel ferrites with enhanced magnetic properties from two intractable metallurgical resources: zinc-bearing dust and nickel laterite ore. *Journal of Superconductivity and Novel Magnetism* **31**, 2655–2660.

Gligorovski, S., Strekowski, R., Barbati, S. & Vione, D. 2015 Environmental implications of hydroxyl radicals ((•)OH). *Chemical Reviews* **115**, 13051–13092.

Ismael, M. 2021 Ferrites as solar photocatalytic materials and their activities in solar energy conversion and environmental protection: a review. *Solar Energy Materials and Solar Cells* **219**, 110786.

Jia, Z., Zhang, W. C., Wang, W. M., Habibi, D. & Zhang, L. C. 2016 Amorphous $Fe_{78}Si_9B_{13}$ alloy: a rapid and reusable photo-enhanced Fenton-like catalyst in degradation of Cibacron Brilliant Red 3B-A dye under UV–vis light. *Applied Catalysis B Environmental* **192**, 46–56.

Jiang, D. N., Chen, M., Wang, H., Zeng, G. M., Huang, D. L., Cheng, M., Liu, Y., Xue, W. J. & Wang, Z. W. 2019 The application of different typological and structural MOFs-based materials for the dyes adsorption. *Coordination Chemistry Reviews* **380**, 471–483.

Kefeni, K. K., Mamba, B. B. & Msagati, T. A. M. 2017 Application of spinel ferrite nanoparticles in water and wastewater treatment: a review. *Separation & Purification Technology* **188**, 399–422.

Kong, L. J., Zhu, Y. T., Liu, M. X., Chang, X. Y., Xiong, Y. & Chen, D. Y. 2016 Conversion of Fe-rich waste sludge into nano-flake Fe-SC hybrid Fenton-like catalyst for degradation of AOII. *Environmental Pollution* **216**, 568–574.

Kostedt, W. L., Drwiega, J., Mazyck, D. W., Lee, S. W., Sigmund, W., Wu, C. Y. & Chadik, P. 2005 Magnetically agitated photocatalytic reactor for photocatalytic oxidation of aqueous phase organic pollutants. *Environmental Science & Technology* **39**, 052–8056.

Kukurugya, F., Vindt, T. & Havlík, T. 2015 Behavior of zinc, iron and calcium from electric arc furnace (EAF) dust in hydrometallurgical processing in sulfuric acid solutions: thermodynamic and kinetic aspects. *Hydrometallurgy* **154**, 20–32.

Liu, S. Q., Feng, L. R., Xu, N., Chen, Z. G. & Wang, X. M. 2012 Magnetic nickel ferrite as a heterogeneous photo-Fenton catalyst for the degradation of rhodamine B in the presence of oxalic acid. *Chemical Engineering Journal* **203**, 432–439.

Lin, X. L., Peng, Z. W., Yan, J. X., Li, Z. Z., Hwang, J. Y., Zhang, Y. B., Li, G. H. & Jiang, T. 2017 Pyrometallurgical recycling of electric arc furnace dust. *Journal of Cleaner Production* **149**, 1079–1100.

Liu, Y., Zhao, Y. & Wang, J. L. 2021 Fenton/Fenton-like processes with in-situ production of hydrogen peroxide/hydroxyl radical for degradation of emerging contaminants: advances and prospects. *Journal of Hazardous Materials* **404**, 124191.

Munoz, M., Pedro, Z. M. D., Casas, J. A. & Rodriguez, J. J. 2015 Preparation of magnetite-based catalysts and their application in heterogeneous Fenton oxidation–a review. *Applied Catalysis B Environmental* **176–177**, 249–265.

National Bureau of Standards 1971 (U.S.) Monoograph 25, V9, P60.

National Bureau of Standards 1981 (U.S.) Monoograph 25, V18, P37.

Neyens, E. & Baeyens, J. 2003 A review of classic Fenton's peroxidation as an advanced oxidation technique. *Journal of Hazardous Materials* **98**, 33–50.

Ramlow, H., Francisco, M. R. A. & Marangoni, C. 2017 Direct contact membrane distillation for textile wastewater treatment: a state of the art review. *Water Science and Technology* **76**, 2565–2579.

Sebag, M. G., Korzenowski, C., Bernardes, A. M. & Vilela, A. C. 2009 Evaluation of environmental compatibility of EAFD using different leaching standards. *Journal of Hazardous Materials* **166**, 670–675.

Shahid, M., Liu, J. L., Ali, Z., Shakir, I., Warsi, M. F., Parveen, R. & Nadeem, M. 2013 Photocatalytic degradation of methylene blue on magnetically separable $MgFe_2O_4$ under visible light irradiation. *Materials Chemistry & Physics* **139**, 566–571.

Su, M. H., He, C., Sharma, V. K., Asi, M. A., Xia, D. H., Li, X. Z., Deng, H. Q. & Xiong, Y. 2012 Mesoporous zinc ferrite: synthesis, characterization, and photocatalytic activity with H_2O_2/visible light. *Journal of Hazardous Materials* **211–212**, 95–103.

Thota, S., Kashyap, S. C., Sharma, S. K. & Reddy, V. R. 2015 Micro Raman, Mossbauer and magnetic studies of manganese substituted zinc ferrite nanoparticles: role of Mn. *Journal of Physics and Chemistry of Solids* **91**, 136–144.

Tu, Y. J., Chang, C. K., You, C. F. & Wang, S. L. 2012 Treatment of complex heavy metal wastewater using a multi-staged ferrite process. *Journal of Hazardous Materials* **209–210**, 379–384.

Vinosha, P. A., Xavier, B., Ashwini, A., Mely, L. A. & Das, S. J. 2017 Tailoring the photo-Fenton activity of nickel ferrite nanoparticles synthesized by low-temperature coprecipitation technique. *Optik-International Journal for Light and Electron Optics* **137**, 244–253.

Wang, H. G., Zhang, M. & Guo, M. 2017 Utilization of Zn-containing electric arc furnace dust for multi-metal doped ferrite with enhanced magnetic property: from hazardous solid waste to green product. *Journal of Hazardous Materials* **339**, 248–255.

Yan, Z. K., Gao, J. M., Li, Y., Zhang, M. & Guo, M. 2015 Hydrothermal synthesis and structure evolution of metal-doped magnesium ferrite from saprolite laterite. *RSC Advances* **5**, 92778–92787.

Zapata, A., Velegraki, T., Sánchez-Pérez, J. A., Mantzavinos, D. & Maldonado, M. I. 2009 Solar photo-Fenton treatment of pesticides in water: effect of iron concentration on degradation and assessment of ecotoxicity and biodegradability. *Applied Catalysis B Environmental* **88**, 448–454.

Zhang, X. Y., Ding, Y. B., Tang, H. Q., Han, X. Y., Zhu, L. H. & Wang, N. 2014 Degradation of bisphenol A by hydrogen peroxide activated with $CuFeO_2$ microparticles as a heterogeneous Fenton-like catalyst: efficiency, stability and mechanism. *Chemical Engineering Journal* **236**, 251–262.

Zhang, D. C., Zhang, X. W., Yang, T. Z., Rao, S., Hu, W., Liu, W. F. & Chen, L. 2017a Selective leaching of zinc from blast furnace dust with mono-ligand and mixed-ligand complex leaching systems. *Hydrometallurgy* **169**, 219–228.

Zhang, H., Liu, J. G., Ou, C. J., Faheem, Shen, J. Y., Yu, H. X., Jiao, Z. H., Han, W. Q., Sun, X. Y., Li, J. S. & Wang, L. J. 2017b Reuse of Fenton sludge as an iron source for $NiFe_2O_4$ synthesis and its application in the Fenton-based process. *Journal of Environmental Sciences* **53** (3), 1–8.

Zhong, Y. H., Liang, X. L., He, Z. S., Tan, W., Zhu, J. X., Yuan, P., Zhu, R. L. & He, H. P. 2014 The constraints of transition metal substitutions (Ti, Cr, Mn, Co and Ni) in magnetite on its catalytic activity in heterogeneous Fenton and UV/Fenton reaction: From the perspective of hydroxyl radical generation. *Applied Catalysis B Environmental*. **s150–151**, 612–618.

Zhou, Y. B., Lu, J., Zhou, Y. & Liu, Y. D. 2019 Recent advances for dyes removal using novel adsorbents: a review. *Environmental Pollution* **252**, 352–365.

First received 28 July 2020; accepted in revised form 30 November 2020. Available online 11 December 2020